BIODIVERSITAS
Volume 26, Number 4, April 2025
Pages: 1691-1697

ISSN: 1412-033X
E-ISSN: 2085-4722
DOI: 10.13057/biodiv/d260419

Gross morphology and osteometry of the ribs of Etawah crossbred goats

SUHARSONO[1], YENI DHAMAYANTI[1], HANA ELIYANI[1], SARMANU[1], LINTANG WINANTYA FIRDAUSY[2,3], SALIPUDIN TASIL MASLAMAMA[4], MUHAMMAD THOHAWI ELZIYAD PURNAMA[2,3,5,♥]

[1]Division of Veterinary Anatomy, Faculty of Veterinary Medicine, Universitas Airlangga. Jl. Dr. Ir. H. Soekarno, Surabaya 60115, East Java, Indonesia
[2]Division of Veterinary Medicine, Department of Health and Life Sciences, Faculty of Health, Medicine, and Life Sciences, Universitas Airlangga. Jl. Wijaya Kusuma No. 113, Giri, Banyuwangi 68425, East Java, Indonesia. Tel.: +62-333-417788, Fax.: +62-333-428890, ♥email: thohawi@fkh.unair.ac.id
[3]Research Group of Animal Biomedical and Conservation, Faculty of Health, Medicine, and Life Sciences, Universitas Airlangga. Jl. Wijaya Kusuma 113, Banyuwangi 68425, East Java, Indonesia
[4]Department of Agricultural Biotechnology, Faculty of Agriculture, Eskişehir Osmangazi Üniversitesi. Eskişehir 26040, Türkiye
[5]Department of Biology, Graduate School of Natural and Applied Sciences, Eskişehir Osmangazi Üniversitesi. Eskişehir 26040, Türkiye.

Manuscript received: 27 January 2025. Revision accepted: 31 March 2025.

Abstract. *Suharsono, Dhamayanti Y, Eliyani H, Sarmanu, Firdausy LW, Maslamama ST, Purnama MTE. 2025. Gross morphology and osteometry of the ribs of Etawah crossbred goats. Biodiversitas 26: 1691-1697.* The ribs have several vital purposes, including protecting the contents of the mediastinum and thoracic cavity, moving superiorly, inferiorly, anteriorly, and posteriorly to aid in breathing, serving as a site for the origin or attachment of certain muscles, and aiding in erythropoiesis during development. However, ribs comprise the first to thirteenth bones with different areas. This study aimed to evaluate the gross anatomy and morphometry of the ribs of Etawah crossbred goats (*Capra aegagrus hircus*) using Multivariate Adaptive Regression Splines (MARS) modeling. A total of 299 ribs from 23 adult male Etawah crossbred cadavers were investigated in this study. Each rib was identified in order from the first to the thirteenth ribs. Rib evaluation was performed on the following i.e., Width of the Tubercle Costochondral (WTC), Width of the Junction Costochondral (WJC), and Length of the Costochondral (LC). Data were calculated using Multivariate Adaptive Regression Splines (MARS) modeling. As a result, gross anatomically, all Etawah crossbred ribs were composed of the costal cartilage at the distal end and the head, neck, and tubercle at the proximal end, shaft, or body. The WTC and WJC sizes revealed an evident decrease from the first to the second rib and then a gradual decrease on the thirteenth rib. Meanwhile, the LC's size revealed a gradual increase from the first to the eighth rib and gradually decreased on the thirteenth rib. In conclusion, using the LC variable, the eighth rib was determined to be a transition location. The eighth rib may be used as a biometric orientation point in the thoracic region since it is identified as the widest bone, particularly for estimating body weight and body condition scores.

Keywords: *Capra aegagrus hircus*, domesticated animals, Etawah crossbred goat, osteometry, ribs configuration

Abbreviations: GCV: Generalized Cross-Validation; LC: Length of the Costochondral; MARS: Multivariate Adaptive Regression Splines; MBF: Maximum number of Basis Functions; MI: Maximum order of Interactions; MO: Maximum Order; WJC: Width of the Junction Costochondral; WTC: Width of the Tubercle Costochondral

INTRODUCTION

Among 34 provinces in Indonesia, there are an estimated 19.22 million goats documented by the Ministry of Agriculture of the Republic of Indonesia (Ditjenpkh 2021), and Etawah crossbred goats (*Capra aegagrus hircus*) are more beneficial since they are more able to survive in extreme circumstances (Hariyono and Endrawati 2023). Despite extreme seasonal changes, the birth rate of Etawah crossbreds reared using traditional methods ranges from 1.84-2.02 litter sizes/year (Amrullah et al. 2023a). Reproductive management is a crucial issue that must be well handled in order to increase reproductive efficiency (Hufana-Duran and Duran 2020). Etawah crossbreds are dual-purpose, meaning they can be used for both meat and milk (Belgania et al. 2023). Etawah crossbreds have large ears, convex facial features, and efficient weight gain (Andaruisworo et al. 2024). In a previous study, intensely reared Etawah crossbreds weighed 43±5.54 kg, semi-intensive 46±1.96 kg, and extensive 49±5.93 kg. Goats have grown intensively measured 74±8.82 cm in length, semi-intensive 74±3.90 cm, and extensive 75±3.61 cm (Nafiu et al. 2020). Compared to the Etawah crossbred, Boer goats similar to Etawah are 10.07% larger in girth at the same age. In addition, generally the entire body of the Boer goat is white, reddish brown in the head area, and has curved horns, thus it can be distinguished from the Etawah crossbred (Nugroho et al. 2018).

Numerous livestock attributes can be evaluated using animal biometrics based on size. Important data for development and reproduction, as well as another characteristic that may alter as a result of diet and environmental influences, may be obtained from these measurements (Acı et al. 2024). Subsequent attempts to estimate the shape of the ribs and thoracic cavity have used one of two broad approaches. The first employs a mix of Principal Component Analysis (PCA) and Generalized Procrustes Analysis (GPA) to measure changes in landmarks across populations. These landmarks are positioned strategically across the thoracic cavity from a series of rib

configurations. In a prior study on human ribs, 106 landmarks from 63 adult male rib cages were analyzed using GPA. The results showed that the rib cage rounded with age (Slice and Stitzel 2004; Gayzik et al. 2008). A prior study in Sahiwal cattle (*Bos taurus* subsp. *indicus* (Linnaeus, 1758)) performed by Khan et al. (2018) employed a similar technique, using a more extensive collection of landmarks throughout the rib cage, to measure heritability estimates of more than 0.70 for height at the back, height at the hook bone, height at the peg bone, and height at the last rib. With this degree of genetic control, Sahiwal cattle's body frames may be sculpted as desired by genetic selection, and selection for specific body measures can be effective (Khan et al. 2018). In another study, the three thoracic measurements of the fifth rib—rib length, thoracic breadth, and dorsal depth—are logarithmically scaled on the anticipated body mass on Old World monkeys, New World monkeys, Hylobates, and Pongo. However, just the fifth rib's trends are a representative example because comparable trends were typically observed at various levels (Kagaya et al. 2008).

It is possible to estimate the goat's weight using rib morphometry. The assumption of chest width and body length can be classified as factors that determine body weight (Purnama et al. 2019). Additionally, the chest cavity is also linked to the goat's capacity for the maximum volume of respiration (Castells et al. 2019). The configuration of the ribs can determine the goat's posture and quality assessment during breeding. The biomechanical activity between muscles and joints develops the ribs' muscular composition and their carcass tenderness traits (Lerch et al. 2023). The widest area in the thoracic region must be revealed by osteometric evaluation because the ribs are composed of the first through thirteenth configurations. In light of the aforementioned problems, this study implemented the Multivariate Adaptive Regression Splines (MARS) modeling approach to evaluate the Width of the Tubercle Costochondral (WTC), Width of the Junction Costochondral (WJC) and Length of the Costochondral (LC) as landmarks for identifying the widest rib in the thoracic region of Etawah crossbred. In particular, the findings of biometric parameters on the ribs can be a landmark for estimating body weight, body condition score, and thorax volume for further application.

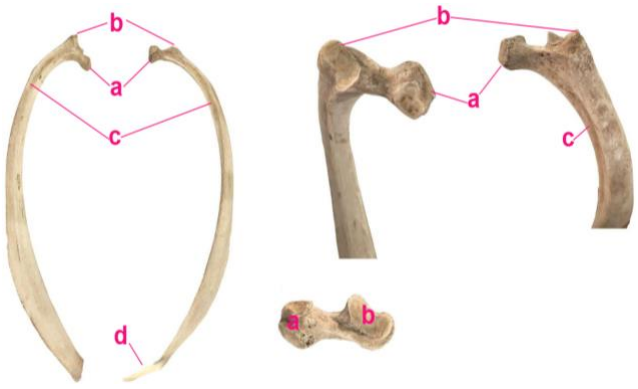

Figure 1. Gross anatomy of the ribs of Etawah crossbred goats: a. Head; b. Tubercle; c. Costal groove; d. Costochondral. WTC parameters were calculated from "a" to "b" points. WJC parameters were calculated between both right and left "d" points. LC parameters were calculated between both medial right and left "c" points

MATERIALS AND METHODS

Ethical approval

Ethical approval is not required because this study did not involve experimental animals and there were no invasive actions on animals. All samples were obtained from the anatomy laboratory, Faculty of Veterinary Medicine, Universitas Airlangga and have been preserved as cadavers that have been fixed in 15% formalin concentration.

Samples

A total of 299 ribs from 23 adult male Etawah crossbred cadavers, aged 18-20 months were investigated. The rib configurations were the serial numbers from the first to the thirteenth rib. Some suspected cadaver samples did not have complete rib numbers due to previous autopsy activities. However, the rib order can be identified based on the connection between the rib head with two articular facets. In order to be easily recognized by the physical characteristics of the head, tubercle, costal groove, angle, and costochondral, the ribs were separated from the remaining muscles, tendons, and fascia. Rib evaluation was performed based on the following parameters, i.e., WTC parameters were observed from the head to the tubercle point, WJC parameters were observed from the costochondral point to the sternal bone, and LC parameters were observed as the distance between the right and left rib costochondral points (Figure 1). The measurement was performed using the tape measure and Vernier caliper Mitutoyo® scale in millimeters (mm).

Data analysis

All parameters were analyzed using MARS modeling. The correlation between rib configurations with WTC, WJC, and LC in MARS modeling was computed on the following equation:

$$f(x) = a_0 + \sum_{m=1}^{M} a_m \prod_{k=1}^{K_M} \left[S_k \left(X_{v(k,m)} - t_k \right) \right]$$

Where:

$f(x)$: Dependent variable of WTC, WJC, and LC

a_m : Coefficient basis function

K_m : Interaction between configuration and position of the ribs

H : *a* step function 1 if $\eta \geq 0$ or 0 if otherwise

S_{km} : The intersection point of the segment (knots) in take on value -1 or +1

t_k : The segment location

X_{v1km} : The predictor variable of ^{K}m

The computational results are represented in figures to reveal the formula of y versus x and determine the optimum punctum of the rib configuration. The optimal statistical model was selected as the one with the lowest Generalized Cross-Validation (GCV) measure, Maximum Order (MO), Maximum order of Interactions (MI), and Maximum number of Basis Functions (MBF).

RESULTS AND DISCUSSION

Gross anatomy of the ribs

A total of 299 ribs from 23 adult male Etawah crossbred goat cadavers, with 157 left ribs and 142 right ribs were identified and then separated from the muscles, tendons, and fascia. Although some ribs were not found completely in the cadavers, the bone configuration could be identified based on the connection between the rib head and the two articular facets (Table 1). The head, neck, and tubercle at the proximal end, shaft, or body, and the costal cartilage at the distal end made up each pair of Etawah crossbred ribs. There were two exterior surfaces and two boundaries on the curving shaft or body. The distal portion was slanted inward, while the top portion had a greater curve. It was discovered that the lateral surface had a broad groove at the top and was convex. It had a concave, smooth medial surface. The posterior border, which housed the costal groove for the intercostal vessels, was convex, whereas the anterior boundary was thick and concave. At the top, this groove was noticeable. Additionally, the head displayed two articular facets, with a costal groove between them. The costo-central articulation was created when these facets were formulated with the facets of the respective vertebrae's bodies. The tubercle was located behind the head, and it was discovered that a narrow section known as the neck divided the two structures. The neck's length was discovered to vary. The entire length of the neck displayed a groove. Except in the series' caudal region, the neck was lengthy and made a closer angle with the shaft or body. Below the rib's main tubercle near the caudal edge of the shaft was an auxiliary tubercle. In the ribs, there was variation in the distance between the two tubercles. Typically, the articular facet of the rib's primary tubercle had a concave form. Variations were noted, nevertheless, in the size and form of the tubercle's facets. This facet formed the costotransverse articulation by connecting with the homologous facet on the thoracic vertebra's transverse process (Figure 1).

The ribs' distal end was slightly enlarged and connected to the costal cartilage. Cylindrical and slightly stretched from side to side, the cartilages were discovered. Both sides' ribs were structurally identical, and there were no gross differences between the sexes. The tubercle of the first rib had a facet that resembled a bicycle seat. At the first rib's proximal portion of the caudal edge, the costal groove was noticeable. Both morphological and anterior attachment to the costal cartilage are used to categorize ribs. Based on their anatomical characteristics, they are categorized as either regular or unusual morphologically. Typical ribs (ribs 3-9) include four main features: a head with two articular facets, a neck, a tubercle, and a shaft. They connect with the spinal column posteriorly and the sternum anteriorly along the costal cartilage. A single rib connects with the axillary spine posteriorly at the costovertebral joint, which has two distinct articulations. First, through two distinct articular facets, the head articulates with the immediately superior and numerically comparable vertebral bodies at the costocorporeal joint. At the costotransverse joint, the tubercle, which is situated where the neck and shaft meet, articulates with the matching vertebral transverse process. Despite a small amount of gliding motion, these joints are naturally stable and support the stability of the thoracic spine (Haase and Shaikh 2024).

Rib evaluation using MARS modeling

According to the MARS modeling, each segment's WTC (Figure 2), WJC (Figure 3), and LC (Figure 4) formed two linear functions in rib configuration. The WTC and WJC sizes revealed an evident decrease from the first to the second rib (WTC: [y = 12.17-2.01x]; WJC: [y = 24.675-6.535x]), and then a gradual decrease on the thirteenth rib (WTC: [y = 8.98-0.24x]; WJC: [y = 14.58-0.64x]) (Table 2, Figures 2-3). Meanwhile, the LC's size revealed a gradual increase from the first to the eighth rib (y = 86.623 + 10.922x) and gradually decreased on the thirteenth rib (y = 269.917-12.136x) (Table 2, Figure 4). It is evident from the osteometric evaluation results that the ribs are arranged in a funnel-like pattern, progressively narrowing to the thirteenth bone after widening from the first to the eighth. In certain animal biometric procedures, the eighth bone—which is arguably the widest punctum in the thoracic region—is used to predict lung volume, body weight, and body score conditions (Smith 2024).

Discussion

A typical technique for detecting each unique rib configuration, characterizing its shape concerning the thoracic cavity, and relating it to body mass estimation is basic osteometry. Several parameters include the use of an ellipse, an arc, a circular ring, and two superimposed arcs to indicate rib shapes (Kindig and Kent 2013; Pratiwi et al. 2024). The ability to completely recreate the underlying rib structure using just the parameters of two recent models has been included. In earlier studies, a seven-parameter model featuring a circle and semi-ellipse connected by short patches was presented (Holcombe et al. 2019). In addition, other study performed by Holcombe et al. (2016) offered the extra advantages of employing specifications that represented themselves as direct geometrical attributes of ribs, such as their size, aspect ratio, and skewness, and simplified the parameter space (with one fewer parameter and joining patches) by using linked spherical as the model primitives. The average geometric qualities from within a population would be reflected in any rib that was constructed implementing statistically average coefficient values.

The motion characteristics of the spine at various slopes were examined using the Qualisys Track Manager (QTM) gait analysis system in conjunction with the Saanen goat's normal gait cycle. It can obtain the changes of the goat spine under actual movement states, which serves as a

reference for the ensuing research on goat movement mechanism, in contrast to the conventional spine biological characteristics analysis method (Zhang et al. 2024). In the meantime, the various directions of the lumbar and thoraco-lumbar vertebral changes were analyzed using the Gaussian Mixture Model (GMM) clustering algorithm. It was discovered that the goat's lumbar and thoraco-lumbar vertebral motion was primarily represented by a left-right swing in the coronal plane, when combined with anatomical knowledge (Zhang et al. 2018). Ultimately, it was determined that the coupling motion of the thoraco-lumbar cooperative motion and the flexible swing of the lumbar vertebrae at the slope of 10° had the most significant effect on the motion stability based on the analysis of the maximin and variation range of the lumbar vertebrae and thoraco-lumbar vertebrae in the central plane. Angle variation data under various slopes were shown to exhibit a clear clustering effect when the covariance matrix was diagonal and when the covariance matrix was different. The primary way that the lumbar and thoracolumbar vertebrae moved in the coronal plane was as a left-right swing (Zhang et al. 2022).

Table 1. Distribution of rib configuration samples in Etawah crossbred goats

Rib no.	Total rib sample	
	Left side	Right side
1	17	17
2	17	14
3	17	13
4	15	13
5	14	13
6	13	12
7	12	11
8	13	11
9	14	13
10	9	6
11	6	5
12	5	4
13	5	10
Total	157	142

Table 2. Osteometry of ribs in Etawah crossbred goats

Ribs no.	WTC (mm)	WJC (mm)	LC (mm)
1	10.41±1.87	17.00±4.04	86.63±11.72
2	8.19±1.82	10.96±1.97	113.62±13.58
3	9.07±3.40	12.07±2.05	126.50±14.77
4	8.33±1.28	12.82±2.69	139.68±14.79
5	7.55±1.29	12.07±2.47	149.68±16.37
6	7.50±1.16	11.64±1.58	155.89±21.24
7	7.08±1.24	10.72±1.83	157.95±20.12
8	6.54±1.27	9.64±1.29	159.89±24.63
9	6.68±0.90	7.92±0.86	164.23±26.86
10	6.71±0.66	6.98±1.45	166.17±29.27
11	6.44±0.60	6.28±2.01	157.33±36.48
12	5.78±0.97	5.48±1.15	133.18±20.02
13	5.09±1.80	5.18±1.72	90.03±37.06

Notes: WTC: Width of the Tubercle Costochondral; WJC: Width of the Junction Costochondral; LC: Length of the Costochondral

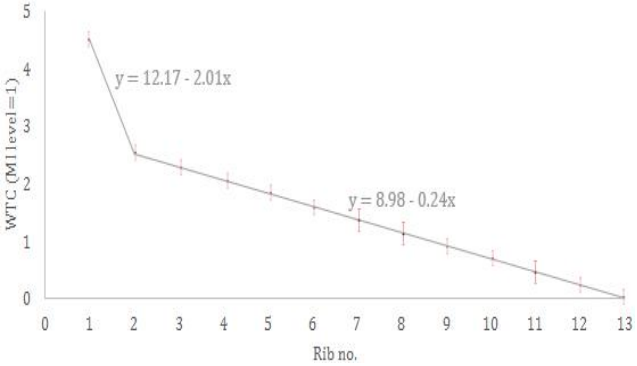

Figure 2. MARS modeling for WTC with MO: 0; MI: 1; MBF: 2; and GCV value: 2.396

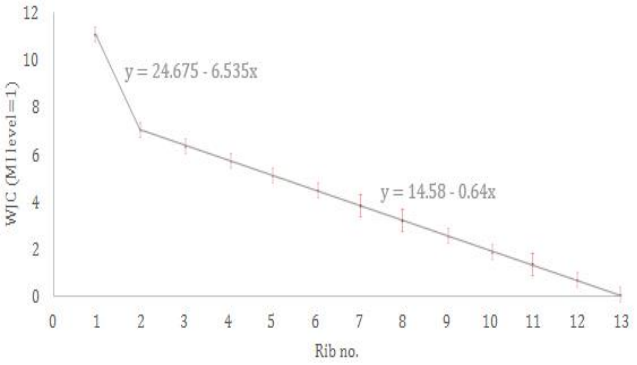

Figure 3. MARS modeling for WJC with MO = 0; MI = 1; MBF = 2; and GCV value = 6.245

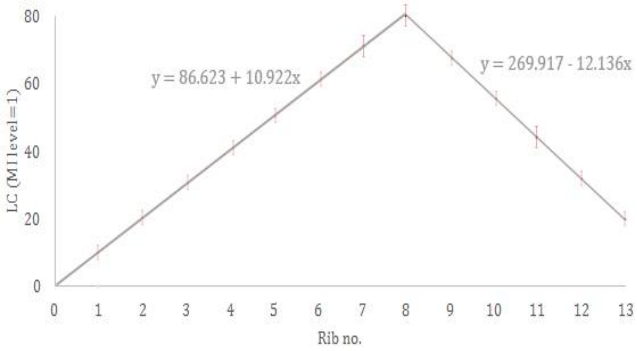

Figure 4. MARS modeling for LC with MO = 0; MI = 1; MBF = 2; and GCV value= 6.245

In graphic models of human cartilage, the seventh rib has the largest punctum pattern, whereas the next rib has the smallest (Joshua et al. 2014). Thirteen pairs of Etawah crossbred goats were used in this study to create a two-segmented linear model. While WTC and WJC share the same pattern and are segmented in the second rib, the LC graph is segmented in the eighth rib. Because the eighth rib represents the boundary and transition point between the sternal and asternal ribs, this study highlighted the morphological characteristics of the Etawah crossbred goat.

In contrast, according to a prior study, the third through tenth ribs are categorized as normal from a morphologic standpoint because they feature articular facets and an extended body that is joined to the rib head by a tubercle and neck. Both of these joints are synovial; the head articulates with the vertebral body to produce the costovertebral joint, while the tubercle articulates with the vertebra's transverse process to form the costotransverse joint. Because they lack traits that the other ribs share, the first, second, eleventh, and twelfth ribs are regarded as unusual. The cervicothoracic junction is characterized by the first and second ribs. The third to tenth ribs are categorized as typical morphologically because they include articular facets and an extended body that is joined to the rib head by a tubercle and neck. The tubercle articulates with the vertebra's transverse process to produce the costotransverse joint, while the head articulates with the vertebral body to form the costovertebral joint. Both of these joints are synovial. Since the first, second, eleventh, and twelfth ribs lack traits that the other ribs share, they are regarded as unusual. The cervicothoracic junction is characterized by the first and second ribs. While the second rib is longer and thinner than the first, it possesses a tuberosity for fastening the anterior serratus muscle. The first rib is wider and shorter, with grooves associated with the subclavian arteries and a tubercle for fixing the scalene muscles. Because they lack a neck, a tubercle, and anterior articular facets, the eleventh and twelfth ribs are uncommon. In order to articulate with the nearby upper vertebral body, the second through ninth ribs have a second articular face on their heads. Each rib contains a lower costal groove that is connected to the intercostal neurovascular bundle (Talbot et al. 2017).

The head (*Caput costae*) and tubercle (*Tuberculum costae*), attached to the spine, form up the proximal ribs. In the *Processus transversus Thoracalis I-XIII*, the *Tuberculum costae* is connected to the joint area (*Fovea costae transversus*). In contrast, the *Caput costae* is connected to the joint area (*Fovea capitis costae cranial et caudal*) (Musil et al. 2018). The epaxial muscles, the most medial vertebrae, and the ribs form the thoracic cavity, and the connection to the two joints is fully closed (Hudson and Hamilton 2017). The joint of cartilage-covered ribs and the sternum bone segment is known as the costochondral junction. According to Srour et al. (2015), the first rib segment's cartilage is bigger, more dense, and shorter than the subsequent rib segment. Five asternal ribs and eight sternal cartilages were observed in this investigation. The anterior rib configurations known as sternal ribs articulate and are joined to the sternum bone directly. Due to their firm attachment to the sternum bone, the first eight sternal ribs are less flexible (Khabyuk et al. 2022). A costal arch is formed by the posterior arrangement of the asternal ribs, which are indirectly attached to the sternum bone. The floating ribs that are not attached to the sternum bone are known as fluctuant ribs. The floating ribs, which are the other atypical ribs, are ribs 11 and 12. Similar to the first rib, they lack a tubercle and comprise a single facet on the head. To simple cartilages, their ends taper. The term floating ribs refers to the cartilage's complete lack of attachment to the rest of the rib cage. Several sheep and goat breeds have fluctuant bones in the last three rib configurations (Farghali et al. 2020). In a previous study, six specimens of adult Blue bulls (*Boselaphus tragocamelus* (Pallas, 1766)) of either sex had their first, second, and third pairs of ribs investigated. They had a head, neck, shaft, or body, tubercle at the proximal end, and costal cartilage at the distal end. On the caudal edge of the shaft, beneath the ribs' main tubercle, was an additional tubercle. In females, the accessory tubercle was located at the caudal boundary 4.1±0.08 cm below the proximal tubercle, while in males, it was 4.2±0.11 cm below. At the second rib's proximal end of the caudal border, the costal groove was noticeable. The second rib lacked the accessory tubercle. At the caudal boundary, the accessory tubercle was located 3.3±0.13 cm below the proximal tubercle in females and 3.5±0.10 cm below it in males. Up to the third rib, the shaft became more curved. There were no gross differences between the sexes, and the ribs on both sides had comparable characteristics. Major variations between the sexes of this species were reflected in the biometrical observations on several parameters of the first, second, and third pairs of ribs of the Blue Bull (Sathapathy et al. 2018).

The superior and inferior angles of the rib are where it curves. They are also attachment points for ligaments and trunk muscles. Additionally, thoracic muscles and connective tissue join to the ribs through the superior and inferior crests, which are elevated edges. A rib's body is its major portion. Intercostal arteries and nerves can travel through the costal grooves inside the ribs, supporting thoracic function. The costovertebral joints are formed by the facets on the heads of the ribs that connect with the thoracic vertebrae (Amrullah et al. 2023b). A conspicuous, rounded projection that connects with the thoracic vertebrae is called the rib head. The costal margins act as attachment points for the thoracic muscles and establish the boundaries of the ribs. The area between the head and the body is called the rib's neck. The sternum or vertebrae articulate with the costal notches. Both articular and nonarticular tubercles are found on the ribs; the latter act as attachment sites for trunk muscles (de Farias et al. 2020).

The external and internal intercostal muscles are based on the ribs. This muscle contributes to the breathing process. According to Wen and Lee (2018), the Serratus ventralis muscles are inserted in the sixth and seventh goat ribs, while the scalenus muscles are inserted in the third and fifth ribs. The asternale rib and xiphoid cartilage serve as attachment points for intercostal muscles and abdominal muscle fibers (Haase and Shaikh 2024). Depending on the rib configuration, the rib shaft's length, width, and number of curves change. The costal arch is shaped more gradually by the longer second rib, while the first rib is shorter and straighter (Levillain et al. 2019). A previous study reported that the chest circumference of Etawah crossbreds reared intensively was 37±7.32 cm, semi-intensive 37±6.31 cm, and extensive 39±5.60 cm (Nafiu et al. 2020). The findings of the earlier study on bone loss with aging are in line with the trends of declining rib bone volume proportion and mineralization with age. Age-related decreases in rib bone volume, rather than an increase in calcification mineral

density, were likely the cause of the mineralization ratio's apparent increase with age. Both calcification mineral density and calcification volume fraction were not well predicted by rib mineral density or rib volume fraction, respectively (Ikeda 2017). It's unclear to what extent costal cartilage calcification may be a compensatory strategy or linked to a shift in stress patterns brought on by a lower rib bone modulus, but both merit more research (Nourin et al. 2024). In our perspective, since the sample of this study was a cadaver, the live goat weight parameter could not be evaluated and correlated with rib morphometry. Whereas this parameter may reveal a regression correlation related to body weight with rib morphometry.

In conclusion, the eighth rib was identified as a transition site based on the LC variable. From the first to the eighth rib, the LC variable steadily grew; from the eighth to the thirteenth rib, it gradually decreased. In the meantime, the WTC and WJC models showed a similar trend. From the first to the thirteenth rib configurations, the WTC and WJC variables gradually displayed a minimizing trend. According to this study, the eighth rib can serve as a reference point for calculating chest girth to assess body weight and body condition score in Etawah crossbred for future applications.

ACKNOWLEDGEMENTS

The authors thank the Dean of the Faculty of Health, Medicine, and Life Sciences and the Dean of the Faculty of Veterinary Medicine, Universitas Airlangga, Indonesia, for supporting facilities during this study. The study did not receive any substantial financing that could have affected its findings, and the authors confirmed no conflicts of interest related to this publication.

REFERENCES

Acı R, Duman E, Kul S, Yiğit S. 2024. Effect of Bone Morphogenetic Protein Receptor-1B (BMPR-1B) gene variant on litter size in Akkaraman sheep breed. J Medik Veteriner 7 (2): 235-243. DOI: 10.20473/jmv.vol7.iss2.2024.235-243.

Amrullah MF, Utomo B, Utama S, Lestari TD, Suprayogi TW, Restiadi TI, Belgania RH, Pakpahan S, Khairullah AR, Kurniawan SC, Silaen OSM, Hasib A. 2023a. Comparison of genetic diversity of LEP gene between Indonesia domestic goats: Etawa cross and Senduro goats. Biodiversitas 24 (12): 6567-6573. DOI: 10.13057/biodiv/d241218.

Amrullah MF, Utomo B, Utama S, Suprayogi TW, Lestari TD, Restiadi TI, Belgania RH. 2023b. Genetic analysis of the leptin gene in goats based on GenBank DNA sequences. Jurnal Medik Veteriner 6 (1): 125-131. DOI: 10.20473/jmv.vol6.iss1.2023.125-131.

Andaruisworo S, Yuniati E, Tanjungsari A, Solikin N, Anifiatiningrum A, Fitriani F. 2024. Performance of Etawa crossbreed (PE) in the colony. J Acad Sci 1 (6): 725-730. DOI: 10.59613/3ckvde15.

Belgania RH, Utomo B, Mustofa I, Kholifah Y, Amrullah MF. 2023. Detection of Melanocortin Receptor Type 4 (MC4R) gene in semen of Etawah crossbreed and Senduro goats. Jurnal Medik Veteriner 6 (2): 209-215. DOI: 10.20473/jmv.vol6.iss2.2023.209-215.

Castells E, Lacasta D, Climent M, Pérez M, Sanromán F, Jiménez C, Ferrer LM. 2019. Diagnostic imaging techniques of the respiratory tract of sheep. Small Rumin Res 180: 112-126. DOI: 10.1016/j.smallrumres.2019.05.021.

de Farias LdPG, Menezes DC, Faé IS, de Arruda PHC, Santos JMMM, da Silva Teles GB. 2020. Anatomical variations and congenital anomalies of the ribs revisited by multidetector computed tomography. Radiol Bra 53 (6): 413-418. DOI: 10.1590/0100-3984.2019.0131.

Ditjenpkh. 2021. Livestock and Animal Health Statistics 2021. Directorate General of Livestock and Animal Health, Ministry of Agriculture of the Republic of Indonesia, Jakarta. [Indonesian]

Farghali HAM, Khatem KKA, Shamaa AA. 2020. Review on the common surgical affections in sheep and goats. J Appl Vet Sci 5 (3): 40-48. DOI: 10.21608/JAVS.2020.98366.

Gayzik FS, Yu MM, Danelson KA, Slice DE, Stitzel JD. 2008. Quantification of age-related shape change of the human rib cage through geometric morphometrics. J Biomech 41 (7): 1545-1554. DOI: 10.1016/j.jbiomech.2008.02.006.

Haase DR, Shaikh HS. 2024. Anatomy of the ribs, sternum, and costal margin. J Orthop Trauma 38: S1-S6. DOI: 10.1097/BOT.0000000000002919.

Hariyono D, Endrawati E. 2023. Indigenous goat genetic resources in Indonesia: Current status and future improvement. J Adv Vet Res 13 (1): 141-149.

Holcombe SA, Kang Y-S, Derstine BA, Wang SC, Agnew AM. 2019. Regional maps of rib cortical bone thickness and cross-sectional geometry. J Anat 235 (5): 883-891. DOI: 10.1111/joa.13045.

Holcombe SA, Wang SC, Grotberg JB. 2016. The effect of rib shape on stiffness. Stapp Car Crash J 60: 11-24. DOI: 10.4271/2016-22-0002.

Hudson LC, Hamilton WP. 2017. Musculoskeletal system. In: Hudson LC, Hamilton WP (eds). Atlas of Feline Anatomy for Veterinarians. Teton NewMedia, Jackson, Wyoming, United States.

Hufana-Duran D, Duran PG. 2020. Animal reproduction strategies for sustainable livestock production in the tropics. IOP Conf Ser: Earth Environ Sci 492: 012065. DOI: 10.1088/1755-1315/492/1/012065.

Ikeda T. 2017. Estimating age at death based on costal cartilage calcification. Tohoku J Exp Med 243 (4): 237-246. DOI: 10.1620/tjem.243.237.

Joshua A, Shetty L, Pare V. 2014. Variations in dimensions and shape of thoracic cage with aging: An anatomical review. Anat J Afr 3 (2): 346-355.

Kagaya M, Ogihara N, Nakatsukasa M. 2008. Morphological study of the anthropoid thoracic cage: Scaling of thoracic width and an analysis of rib curvature. Primates 49: 89-99. DOI: 10.1007/s10329-007-0064-z.

Khabyuk J, Pröls F, Draga M, Scaal M. 2022. Development of ribs and intercostal muscles in the chicken embryo. J Anat 241 (3): 831-845. DOI: 10.1111/joa.13716.

Khan MA, Khan MS, Waheed A. 2018. Morphological measurements and their heritabilities for Sahiwal cattle in Pakistan. J Anim Plant Sci 28 (2): 431-440.

Kindig MW, Kent RW. 2013. Characterization of the centroidal geometry of human ribs. J Biomech Eng 135: 111007. DOI: 10.1115/1.4025329.

Lerch S, Morel I, Dohme-Meier F, Le Cozler Y, Xavier C. 2023. Estimation of body and carcass composition of crossbred growing bulls from 11th rib dissection. Anim Open Space 2: 100030. DOI: 10.1016/j.anopes.2022.100030.

Levillain A, Rolfe RA, Huang Y, Iatridis JC, Nowlan NC. 2019. Short-term foetal immobility temporally and progressively affects chick spinal curvature and anatomy and rib development. Eur Cells Mater 37: 23-41. DOI: 10.22203/ecm.v037a03.

Musil V, Blankova A, Baca V. 2018. A plea for an extension of the anatomical nomenclature: The locomotor system. Bosn J Basic Med Sci 18 (2): 117-125. DOI: 10.17305/bjbms.2017.2276.

Nafiu LO, Pagala MA, Mogiye SL. 2020. Karakteristik produksi kambing peranakan Etawa dan kambing Kacang pada sistem pemeliharaan berbeda di Kecamatan Toari, Kabupaten Kolaka. Jurnal Ilmu Produksi dan Teknologi Hasil Peternakan 8: 91-96. DOI: 10.29244/jipthp.8.2.91-96. [Indonesian]

Nourin S, bin Mohit MM, Zohara BF, Islam MF. 2024. Ovum pick-up and ovaries characterization of Black Bengal goat from slaughterhouse. Jurnal Medik Veteriner 7 (2): 219-227. DOI: 10.20473/jmv.vol7.iss2.2024.219-227.

Nugroho T, Nurhidayati A, Ayuningtyas AI, Kustiyani C, Prastowo S, Widyas N. 2018. Birth and weaning weight of kids from different Boer goat crosses. IOP Conf Ser: Earth Environ Sci 142: 012010. DOI: 10.1088/1755-1315/142/1/012010.

Pratiwi H, Putra DP, Septian WA, Furqon A, Suyadi S. 2024. Macroanatomy, histomorphometry, and androgen receptor expression in the epididymis of Kacang goats aged 4, 8, and 12 months. Jurnal Medik Veteriner 7: 300-309. DOI: 10.20473/jmv.vol7.iss2.2024.300-309.

Purnama MTE, Dewi WK, Prayoga SF, Triana NM, Aji BSP, Fikri F, Hamid IS. 2019. Preslaughter stress in Banyuwangi cattle during transport. Indian Vet J 96 (12): 50-52.

Sathapathy S, Dhote BS, Mahanta D, Tamilselvan S, Singh I, Mrigesh M, Joshi SK. 2018. Gross morphological and biometrical sexual dimorphic studies on the first, second and third pairs of ribs of Blue bull (*Boselaphus tragocamelus*). J Anim Res 8 (6): 1041-1046. DOI: 10.30954/2277-940X.12.2018.15.

Slice DE, Stitzel J. 2004. Landmark-based geometric morphometrics and the study of allometry. SAE Trans 113 (1): 199-207.

Smith D. 2024. Anatomy and postmortem examination. In: Schmidt RE, Struthers JD, Phalen DN (eds). Pathology of Pet and Aviary Birds. 3rd Eds. John Wiley & Sons, Inc., Hoboken, New Jersey. DOI: 10.1002/9781119650522.ch1.

Srour MK, Fogel JL, Yamaguchi KT, Montgomery AP, Izuhara AK, Misakian AL, Lam S, Lakeland DL, Urata MM, Lee JS, Mariani FV. 2015. Natural large-scale regeneration of rib cartilage in a mouse model. J Bone Miner Res 30 (2): 297-308. DOI: 10.1002/jbmr.2326.

Talbot BS, Gange Jr CP, Chaturvedi A, Klionsky N, Hobbs SK, Chaturvedi A. 2017. Traumatic rib injury: Patterns, imaging pitfalls, complications, and treatment. Radiographics 37 (2): 628-651. DOI: 10.1148/rg.2017160100.

Wen M-H, Lee K-Z. 2018. Diaphragm and intercostal muscle activity after mid-cervical spinal cord contusion in the rat. J Neurotrauma 35 (3): 533-547. DOI: 10.1089/neu.2017.5128.

Zhang F, Cui X, Wang S, Sun H, Wang J, Wang X, Fu S, Guo Z. 2022. Analysis of kinematic characteristics of saanen goat spine under multi-slope. Biomimetics 7 (4): 181. DOI: 10.3390/biomimetics7040181.

Zhang F, Wang X, Cui X, Qiu Y, Teng S, Ali S, Fu S. 2024. Analysis of mechanical properties of functional parts of goat hoofs under multi-slope. Agriculture 14 (3): 451. DOI: 10.3390/agriculture14030451.

Zhang F, Zheng L, Wang W, Wang Y, Wang J. 2018. Development of agricultural bionic mechanisms: Investigation of the effect of joint angle and pressure on the stability of goats moving on sloping lands. Intl J Agric Biol Eng 11: 35-41. DOI: 10.25165/j.ijabe.20181103.3633.